JOURNAL OF NATURAL PRODUCTS

pubs.acs.org/jnp

Article

Emerimicins V−X, 15-Residue Peptaibols Discovered from an *Acremonium* sp. through Integrated Genomic and Chemical Approaches

Guangwei Wu, Bryn T. M. Dentinger, Jason R. Nielson, Randall T. Peterson, and Jaclyn M. Winter*

Cite This: *J. Nat. Prod.* 2021, 84, 1113−1126

Read Online

ACCESS | Metrics & More | Article Recommendations | Supporting Information

ABSTRACT: Fermentation of *Acremonium tubakii* W. Gams isolated from a soil sample collected from the University of Utah led to the isolation and characterization of six new linear pentadecapeptides, emerimicins V−X (**1**−**6**). Peptaibols containing 15-residues are quite rare, with only 22 reported. Genome mining and bioinformatic analysis were used to identify the emerimicin 60 kbp *eme* biosynthetic cluster harboring a single 16-module hybrid polyketide-nonribosomal peptide synthetase. A detailed bioinformatic investigation of the corresponding 15 adenylation domains, combined with 1D and 2D NMR experiments, LC-MS/MS data, and advanced Marfey's method, allowed for the elucidation and absolute configuration of all proteinogenic and nonproteinogenic amino acid residues in **1**−**6**. As some peptaibols possess cytotoxic activity, a zebrafish embryotoxicity assay was used to evaluate the toxicity of the six emerimicins and showed that emerimicin V (**1**) and VI (**2**) exhibit the most potent activity. Additionally, out of the six emerimicins, **1** displayed modest activity against *Enterococcus faecalis*, methicillin-resistant *Staphylococcus aureus*, and vancomycin-resistant *Enterococcus faecium* with MIC values of 64, 32, and 64 μg/mL, respectively.

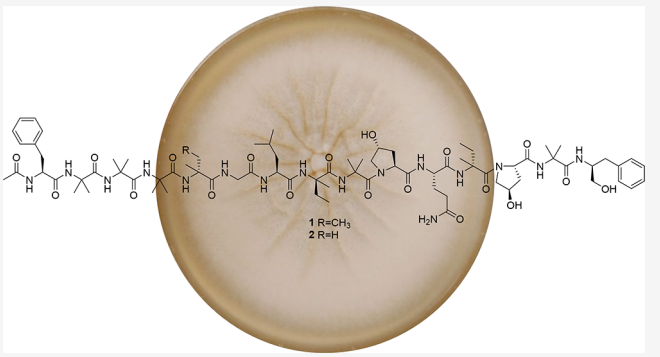

Nonribosomal peptides are a diverse class of biologically active metabolites containing amino-acid-derived moieties. Many of the antibiotics used today such as the penicillins, cephalosporins, vancomycin, and echinocandins are peptide-derived and are biosynthesized by multidomain and multimodular nonribosomal peptide synthetases (NRPS).[1] Peptaibols are nonribosomally biosynthesized peptides predominantly produced by filamentous fungi belonging to the order Hypocreales.[2−4] Their structures are generally linear and amphipathic and contain a high proportion of α,α-dialkylated α-amino acids, such as α-aminoisobutryic acid (Aib) and isovaline (Iva).[5−7] Peptaibols range in length from 5 to 22 amino acids and, in addition to containing α,α-dialkylated α-amino acid residues, feature a high proportion of nonproteinogenic amino acids, an acetylated N-terminus, and a C-terminal amino alcohol.[4,8] Peptaibols possess a variety of biological activities including anticancer, antibacterial, antifungal, and antiviral,[2,9] and the presence of Aib residues has been shown to promote α-helical and 3_{10}-helical conformations, which provides this class of peptides with their unique ability to form pores or channels in lipid membranes.[10,11] In an effort to discover new anti-infective agents from filamentous fungi, we focused our efforts on a culture of *Acremonium tubakii* W. Gams exhibiting potent antimicrobial activity against methicillin-resistant *Staphylococcus aureus*, *Enterococcus faecalis*, and vancomycin-resistant *Enterococcus faecium*. Using bioactivity-guided fractionation coupled with genome mining, bioinformatic, and chemical approaches, we report the isolation and characterization of six new 15-residue peptaibols, emerimicins V−X (**1**−**6**), including the absolute configurations for all amino acid residues. Additionally, we describe the identification of the 60 kb emerimicin biosynthetic cluster and bioinformatic analysis of the 15 adenylation domains within the polyketide synthase (PKS)-NRPS EmeB.

RESULTS AND DISCUSSION

Soil samples were collected from the University of Utah campus, and fungal isolates were identified using ITS sequencing. The strains were then cultured under a variety of media conditions, and after cultivation in PDB media, the crude extract of *A. tubakii* showed 100% inhibition against several pathogenic bacteria at a concentration of 100 μg/mL.

Received: October 28, 2020
Published: February 22, 2021

https://dx.doi.org/10.1021/acs.jnatprod.0c01186
J. Nat. Prod. 2021, 84, 1113−1126

Chart 1

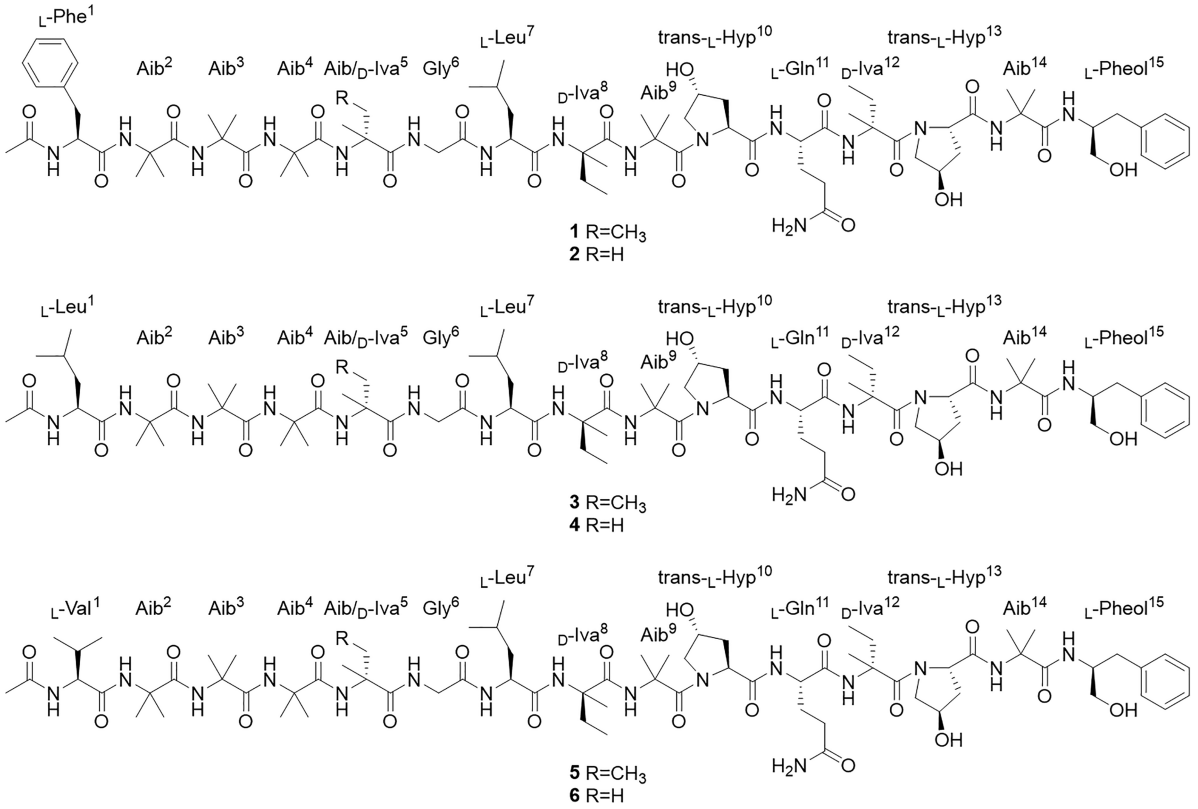

To aid in the dereplication of known antibiotics produced by this *Acremonium* strain, we employed genomic and bioinformatic approaches to identify potential biosynthetic gene clusters that could be responsible for the observed activity. The 38 Mbp genome of *A. tubakii* was sequenced and assembled, and genome mining revealed 44 putative biosynthetic clusters. With the exception of the biosynthetic cluster that synthesizes the antibacterial nortriterpene helvolic acid,[12] no other previously characterized antibiotic-producing clusters were identified in the genome. Interestingly, out of the 44 total biosynthetic clusters, 22 contained NRPSs, of which two appeared to be peptaibol-related. A closer inspection of the modules and domain organization within the NRPS megasynthetases suggested that one of the peptaibol clusters would be making a decapeptide, whereas the other cluster would biosynthesize a pentadecapeptide. Mass spectrometry profiling of the crude extract revealed six peptides with $m/z > 1500$ Da. As 15 amino acid residue peptaibols are rare (Table S1), we set out to isolate the peptides and evaluate their antibiotic activity, as well as their toxicity effects on zebrafish embryos.

A scaled-up fermentation of the fungal strain with HP-20 resin, followed by solvent extraction and partitioning, normal phase chromatography, and bioactivity-guided fractionation with reverse phase chromatography, yielded six acyclic pentadecapeptides, emerimicins V–X (**1**–**6**), as well as the previously described antibacterial agent helvolic acid.[13] Emerimicin V (**1**) was isolated as a white powder, and its molecular formula of $C_{78}H_{122}N_{16}O_{19}$ was determined by HRESI(+)MS. When analyzing the ^{1}H NMR data of **1** (Table 1), clustered amino acid α proton signals (δ_H 3.2–4.3 ppm) and exchangeable amide proton signals (δ_H 7.0–8.8 ppm) were observed, indicating a peptide structure. Additionally, the 1D NMR revealed 16 amide carbonyl carbon bonds (δ_C 170–177), suggesting a 15–16 amino acid residue peptide. TOCSY and COSY spin systems, coupled with HMBC correlations, enabled us to identify the four proteinogenic amino acids Phe, Gly, Leu, and Gln and 11 nonproteinogenic amino acids including two 4-hydroxy-proline (Hyp) residues, three Iva residues, five Aib residues, and a C-terminal phenylalaninol (Pheol). HMBC correlations between the NH signal at 8.29 ppm and methyl group at 1.83 ppm, as well as with the carbonyl carbon at 170.9 ppm, confirmed the N-terminus was acetylated. To establish the sequence of the 15 amino acid residues, NOESY and ROESY data showed sequential and long-range NOE correlations between NH-1 (8.29 ppm, Phe), NH-2 (8.59 ppm, Aib^2), NH-3 (7.63 ppm, Aib^3), NH-4 (7.73 ppm, Aib^4), NH-5 (7.50 ppm, Iva^5), NH-6 (7.95 ppm, Gly^6), NH-7 (7.74 ppm, Leu^7), NH-8 (7.40 ppm, Iva^8), NH-9 (7.60 ppm, Aib^9), and 2H-5 (3.51 and 3.73 ppm, Hyp^{10}), suggesting a partial Phe-Aib-Aib-Aib-Iva-Gly-Leu-Iva-Aib-Hyp sequence. Additional key NOE correlations between 2H-3 (1.77 and 2.16 ppm, Hyp^{10}), NH-10 (7.87 ppm, Gln^{11}), NH-11 (7.46 ppm, Iva^{12}), and 2H-5 (3.64 and 3.39 ppm, Hyp^{13}) suggested the partial sequence Hyp-Gln-Iva-Hyp, whereas the correlations between 2H-3 (1.66 and 2.09 ppm, Hyp^{13}), NH-12 (7.50 ppm, Aib^{14}), and NH-13 (6.97 ppm, Pheol^{15}) suggested a Hyp-Aib-Pheol fragment. Altogether, the NOE correlations coupled with HMBC data allowed us to assign the sequence of the 15 amino acid residues as *N*-Ac-Phe^1-Aib^2-Aib^3-Aib^4-Iva^5-Gly^6-Leu^7-Iva^8-Aib^9-Hyp^{10}-Gln^{11}-Iva^{12}-Hyp^{13}-Aib^{14}-Pheol^{15} (Figure 1 and Tables 1 and S2). Finally, both 4-hydroxy-proline residues were shown to be *trans* based on strong NOE correlations between H$_\alpha$ (δ_H 4.37 for Hyp^{10}; δ_H 4.20 for Hyp^{13}) and H$_\beta$ (δ_H 2.16 for Hyp^{10}; δ_H 2.09 for Hyp^{13}), as well as strong correlations between H$_\gamma$ (δ_H 4.28 for Hyp^{10}; δ_H 4.21 for Hyp^{13}) and H$_\beta$ (δ_H 1.77 for Hyp^{10};

https://dx.doi.org/10.1021/acs.jnatprod.0c01186
J. Nat. Prod. 2021, 84, 1113–1126

Table 1. NMR Spectroscopic Data for Emerimicin V (1) and Emerimicin VI (2) in DMSO-d_6

1				2			
unit	position	δ_C	δ_H (J in Hz)	unit	position	δ_C	δ_H (J in Hz)
Ac	1	170.9 C		Ac	1	170.9 C	
	2	22.8 C	1.83, s		2	22.8 C	1.83, s
Phe[1]	1	172.9 C		Phe[1]	1[a]	172.9C	
	2	55.7 CH	4.33, m		2	55.6 CH	4.33, m
	3	36.8CH_2	2.84, dd (9.3, 14.0); 2.96, dd (9.3, 14.0)		3[b]	36.9.0 CH_2	2.84, dd (9.0, 14.0); 2.96, dd (9.0, 14.0)
	4	137.9 C			4	137.9 C	
	5/5′	129.6 CH	7.29, overlap		5/5′	129.7 CH	7.29, overlap
	6/6′	128.6 CH	7.29, overlap		6/6′	128.6 CH	7.29, overlap
	7	126.9 CH	7.22, overlap		7	126.9 CH	7.22, overlap
	NH		8.29, d (6.1)		NH		8.29, d (5.9)
Aib[2]	1[a]	175.3 C		Aib[2]	1[c]	176.1 C	
	2[b]	56.5 C			2[d]	56.4 C	
	3	24.2 CH_3	1.26, s		3	24.1 CH_3	1.27, s
	4	23.9 CH_3	1.31, s		4[e]	23.9 CH_3	1.32, s
	NH		8.59, s		NH		8.59, s
Aib[3]	1[a]	175.6 C		Aib[3]	1[c]	176.1 C	
	2[b]	56.3 C			2[d]	56.4 C	
	3[c]	24.6 CH_3	1.31, s		3	24.6 CH_3	1.31, s
	4[d]	25.1 CH_3	1.29, s		4[f]	25.0 CH_3	1.37, s
	NH		7.63, s		NH		7.65, s
Aib[4]	1	176.6 C		Aib[4]	1[g]	175.6 C	
	2[b]	56.3 C			2[d]	56.4 C	
	3[d]	25.1 CH_3	1.37, s		3[f]	25.1 CH_3	1.37, s
	4	25.7 CH_3	1.28, s		4	25.4 CH_3	1.28, s
	NH		7.73, s		NH		7.69, s
Iva[5]	1[e]	176.1 C		Aib[5]	1[g]	175.4 C	
	2	59.5 C			2[d]	56.3 C	
	3[f]	28.3 CH_2	1.73, m; 2.21, m		3[f]	25.5 CH_2	1.39, s
	4	8.0 CH_3	0.78, t (6.0)		4	25.9 CH_3	1.28, s
	5	21.7 CH_3	1.34, s		NH		7.57, s
	NH		7.50, s				
Gly[6]	1	171.2 C		Gly[6]	1[h]	174.3 C	
	2	43.8 CH_2	3.63, m; 3.76, m overlap		2	44.0 CH_2	3.63, m; 3.76, m overlap
	NH		7.95, t (6.1)		NH		7.99, t (4.9)
Leu[7]	1[e]	176.0 C		Leu[7]	1	173.6 C	
	2	53.6 CH	4.02, m		2	53.7 CH	4.02, m
	3	39.9 CH_2	1.53, m; 1.69, m		3	39.9 CH_2	1.53, m; 1.69, m
	4[c]	24.6 CH	1.69, m		4	24.6 CH	1.69, m
	5	22.1 CH_3	0.84, d (5.8)		5	22.1 CH_3	0.85, d (6.1)
	6	23.1 CH_3	0.91, d (6.2)		6	23.1 CH_3	0.91, d (5.9)
	NH		7.74, d (5.7)		NH		7.75, d (5.7)
Iva[8]	1[g]	174.3 C		Iva[8]	1[a]	172.9 C	
	2	59.9 C			2	59.8 C	
	3[f]	28.5 CH_2	2.13, m; 1.74, m		3	28.5 CH_2	2.13, m; 1.74, m
	4	7.8 CH_3	0.73, t (7.1)		4	7.8 CH_3	0.73, t (7.0)
	5	22.4 CH_3	1.27, s		5	22.5 CH_3	1.28, s
	NH		7.40, s		NH		7.38, s
Aib[9]	1[g]	174.0 C		Aib[9]	1[h]	174.0 C	
	2[b]	56.7 C			2[d]	56.7 C	
	3	26.3 CH_3	1.35, s		3	26.2 CH_3	1.36, s
	4	23.6 CH_3	1.48, s		4	23.6 CH_3	1.49, s
	NH		7.60, s		NH		7.59, s
Hyp[10]	1[h]	172.4 C		Hyp[10]	1[a]	172.6 C	
	2	61.5 CH	4.37, t (8.7)		2	61.5 CH	4.38, t (8.8)
	3	37.3 CH_2	1.77, m; 2.16, m		3	37.3 CH_2	1.77, m; 2.16, m
	4[i]	69.5 CH	4.28, brs		4[i]	69.4 CH	4.29, brs
	5[b]	56.7 CH_2	3.51, m; 3.73, m		5[d]	56.7 CH_2	3.51, m; 3.73, m

https://dx.doi.org/10.1021/acs.jnatprod.0c01186
J. Nat. Prod. 2021, 84, 1113−1126

Table 1. continued

		1			2		
unit	position	δ_C	δ_H (J in Hz)	unit	position	δ_C	δ_H (J in Hz)
Gln[11]	1	173.6 C		Gln[11]	1[a]	172.4 C	
	2[j]	52.9 CH	4.11, overlap		2[j]	52.9 CH	4.11, t (9.4)
	3	27.2 CH_2	1.88, overlap;		3	27.2 CH_2	1.88, overlap;
			2.13, m				2.15, m
	4	32.0 CH_2	2.11, m		4	32.0 CH_2	2.12, m
	5	172.6 C			5	172.3 C	
	NH		7.87, d (8.4)		NH		7.88, d (8.7)
Iva[12]	1[h]	172.2 C		Iva[12]	1	171.9 C	
	2	58.7 C			2	58.7 C	
	3	27.9 CH_2	2.18, m; 1.69, m		3	27.9 CH_2	2.22, m; 1.69, m
	4	7.4 CH_3	0.72, t (7.5)		4	7.4 CH_3	0.73, t (7.0)
	5	20.3 CH_3	1.39, s		5	20.3 CH_3	1.41, s
	NH		7.46, s		NH		7.47, s
Hyp[13]	1[h]	172.0 C		Hyp[13]	1	171.2 C	
	2	62.4 CH	4.20, overlap		2	62.4 CH	4.20, t (8.8)
	3[k]	37.0 CH_2	1.66, m; 2.09, m		3[b]	37.0 CH_2	1.66, m; 2.09, m
	4[i]	69.5 CH	4.21, brs		4[i]	69.5 CH	4.22, brs
	5	57.3 CH_2	3.64, overlap;		5	57.3 CH_2	3.64, dd (5.3, 18.3);
			3.39, m				3.39, m
Aib[14]	1[g]	174.2 C		Aib[14]	1[h]	174.2 C	
	2[b]	56.5 C			2[d]	56.5 C	
	3	27.3 CH_3	1.15, s		3	27.3 CH_3	1.16, s
	4	25.4 CH_3	1.35, s		4[e]	23.9 CH_3	1.31, s
	NH		7.50, s		NH		7.50, s
Pheol[15]	1	63.8 CH	3.30, dd (7.2, 11.1);	Pheol[15]	1	63.8 CH	3.31, dd (7.2, 11.1);
			3.38, overlap				3.38, overlap
	2[j]	52.9 CH	3.87, m		2[j]	52.9 CH	3.88, m
	3[k]	37.0 CH_2	2.54, overlap;		3[b]	37.0 CH_2	2.53, overlap;
			2.97, dd (14.2, 7.4)				2.94, dd (14.3, 4.2)
	4	139.7 C			4	139.7 C	
	5/5′	129.5 CH	7.18, m overlap		5/5′	129.5 CH	7.18, m overlap
	6/6′	128.3 CH	7.20, m overlap		6/6′	128.3 CH	7.20, m overlap
	7	126.2 CH	7.11, t (6.0)		7	126.2 CH	7.11, t (6.0)
	NH		6.97, d (8.9)		NH		6.97, d (8.9)

[a−k]The carbon chemical shifts are interchangeable, respectively.

δ_H 1.66 for Hyp[13]) (Figure 1). The sequence order of **1** was further supported by the ESIMS/MS data (Figures 2 and S16−S18). A sequence similarity search revealed that the planar structure of **1** is similar to emerimicin IV, a 15 amino acid residue-containing peptaibol isolated from the marine-derived *Emericellopsis minima* Stolk.[14] The key differences are that Val[5] and Aib[8] in emerimicin IV are replaced by two Iva residues in **1**.

The molecular formula for emerimicin VI (**2**) was determined to be $C_{78}H_{122}N_{16}O_{19}$ based on the HRESI(+)MS. Comparing the 1D NMR data for **2** with **1** revealed their structural similarity. The only significant difference was replacement of resonances for the Iva[5] residue with those indicative of Aib, particularly the replacement of $\delta_{H/C}$ 0.78, 8.0 ppm for C-4 with new signals at δ_C 56.3 ppm for C-2, $\delta_{H/C}$ 25.5, 1.39 ppm for C-3, and $\delta_{H/C}$ 25.9, 1.28 ppm for C-4 (Tables 1 and S3). HMBC and NOE correlations confirmed the replacement of Iva[5] with an Aib residue in **2** (Figure 1), and comprehensive NOE and HMBC correlations coupled to ESIMS/MS analysis (Figure 2) established the order of amino acids as *N*-Ac-Phe[1]-Aib[2]-Aib[3]-Aib[4]-Aib[5]-Gly[6]-Leu[7]-Iva[8]-Aib[9]-Hyp[10]-Gln[11]-Iva[12]-Hyp[13]-Aib[14]-Pheol[15].

HRESI(+)MS analysis of emerimicin VII (**3**) and emerimicin VIII (**4**) provided the molecular formulas $C_{75}H_{124}N_{16}O_{19}$ and $C_{74}H_{122}N_{16}O_{19}$, respectively. In contrast to **1**, NMR data for **3** showed the replacement of NMR resonances of a Phe residue with those for Leu (Tables 2 and S4). Comparing NMR data of **4** with those of **3** revealed the replacement of resonances for Iva[5] found in **3** with those for an Aib residue (Tables 2 and S5). Based on ESIMS/MS analysis and NOE and HMBC correlations, the order of amino acid residues was assigned as *N*-Ac-Leu[1]-Aib[2]-Aib[3]-Aib[4]-Iva[5]-Gly[6]-Leu[7]-Iva[8]-Aib[9]-Hyp[10]-Gln[11]-Iva[12]-Hyp[13]-Aib[14]-Pheol[15] for **3** and *N*-Ac-Leu[1]-Aib[2]-Aib[3]-Aib[4]-Aib[5]-Gly[6]-Leu[7]-Iva[8]-Aib[9]-Hyp[10]-Gln[11]-Iva[12]-Hyp[13]-Aib[14]-Pheol[15] for **4** (Figures 1 and 2).

The molecular formulas of emerimicin XI (**5**) and emerimicin X (**6**) were assigned by HRESI(+)MS as $C_{74}H_{122}N_{16}O_{19}$ and $C_{73}H_{120}N_{16}O_{19}$, respectively. NMR data showed that with the exception of the first amino acid residue, **5** was structurally similar to **3**, while **6** was structurally similar **4**. In **3**, the first amino acid residue is Leu, whereas Val is found in **5** (Tables 3 and S6). While both **6** and **5** contain an N-terminal Val residue, NMR data revealed the resonances for Iva[5] in **5** were replaced by those for Aib (Tables 3 and S7). Using a combination of ESIMS/MS analysis and NOE and

https://dx.doi.org/10.1021/acs.jnatprod.0c01186
J. Nat. Prod. 2021, 84, 1113−1126

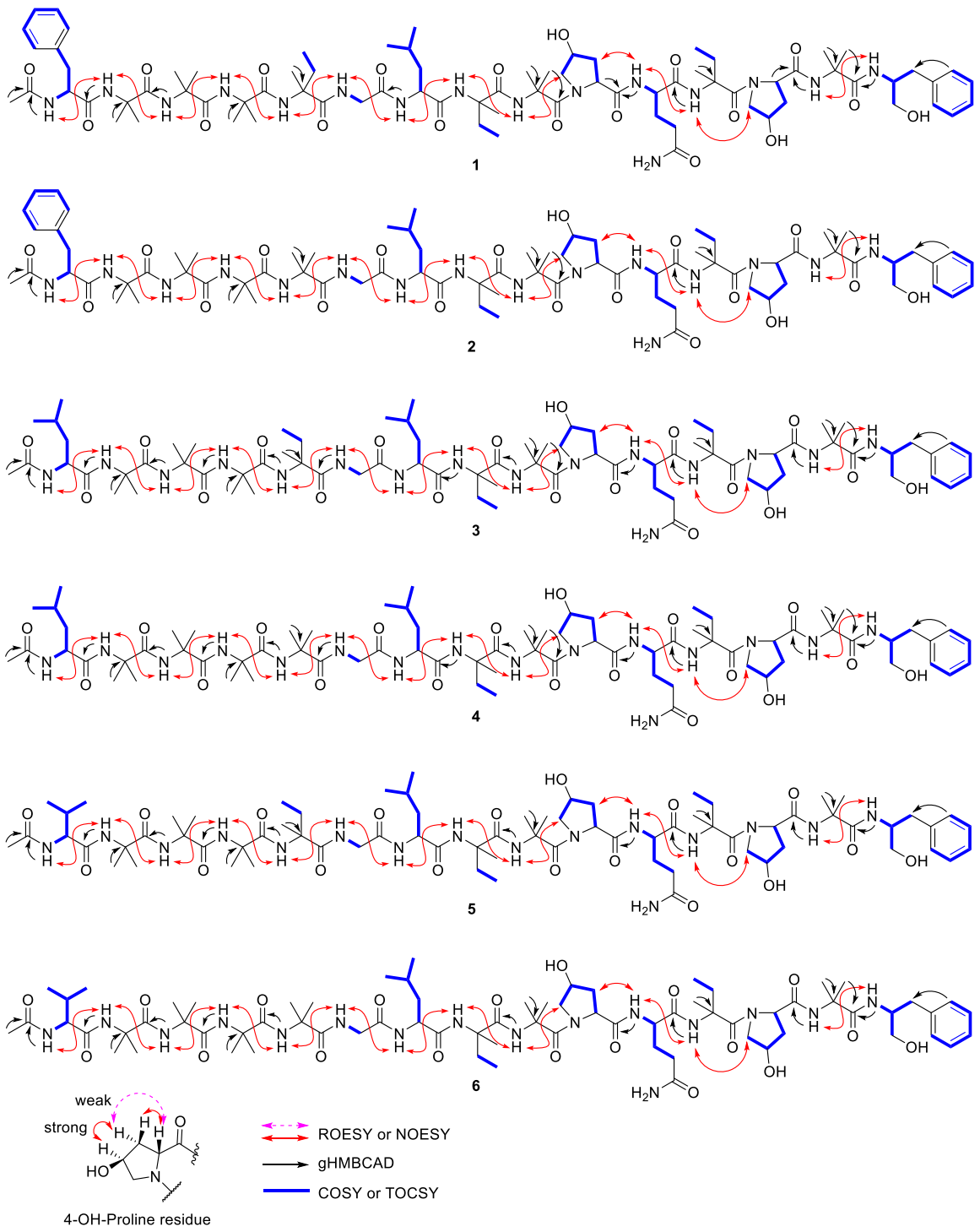

Figure 1. Key 2D NMR correlations for emerimicins V−X (**1**−**6**).

HMBC correlations, the sequence of amino acid residues in **5** was confirmed to be *N*-Ac-Val[1]-Aib[2]-Aib[3]-Aib[4]-Iva[5]-Gly[6]-Leu[7]-Iva[8]-Aib[9]-Hyp[10]-Gln[11]-Iva[12]-Hyp[13]-Aib[14]-Pheol[15] and *N*-Ac-Val[1]-Aib[2]-Aib[3]-Aib[4]-Aib[5]-Gly[6]-Leu[7]-Iva[8]-Aib[9]-Hyp[10]-Gln[11]-Iva[12]-Hyp[13]-Aib[14]-Pheol[15] for **6** (Figures 1 and 2).

To determine the absolute configuration of amino acid residues in **1**−**6**, advanced Marfey's method was performed.[15,16] Each hydrolysate of **1**−**6** was divided into two fractions and derivatized with either 1-fluoro-2,4-dinitrophenyl-5-D,L-leucinamide (D,L-FDLA) or 1-fluoro-2,4-dinitrophenyl-5-L-leucinamide (L-FDLA). Amino acid standards were also derivatized using the same procedure. The D,L-FDLA- or L-FDLA-derived products were monitored by LC-MS. For compounds **1**−**6**, D-Iva, L-Phe, L-Leu, L-Val, L-Gln, *trans*-4-hydroxy-L-Pro, and L-Pheol were deduced after comparing retention times to commercially available standards (Figures S76). With this information, the amino acid configurations for emerimicins V−X were determined to be *N*-Ac-L-Phe[1]-Aib[2]-Aib[3]-Aib[4]-D-Iva[5]-Gly[6]-L-Leu[7]-D-Iva[8]-Aib[9]-*trans*-L-Hyp[10]-L-Gln[11]-D-Iva[12]-*trans*-L-Hyp[13]-Aib[14]-L-Pheol[15] for **1**, *N*-Ac-L-Phe[1]-Aib[2]-Aib[3]-Aib[4]-Aib[5]-Gly[6]-L-Leu[7]-D-Iva[8]-Aib[9]-*trans*-L-Hyp[10]-L-Gln[11]-D-Iva[12]-*trans*-L-Hyp[13]-Aib[14]-L-Pheol[15] for **2**, *N*-Ac-L-Phe[1]-

https://dx.doi.org/10.1021/acs.jnatprod.0c01186
J. Nat. Prod. 2021, 84, 1113−1126

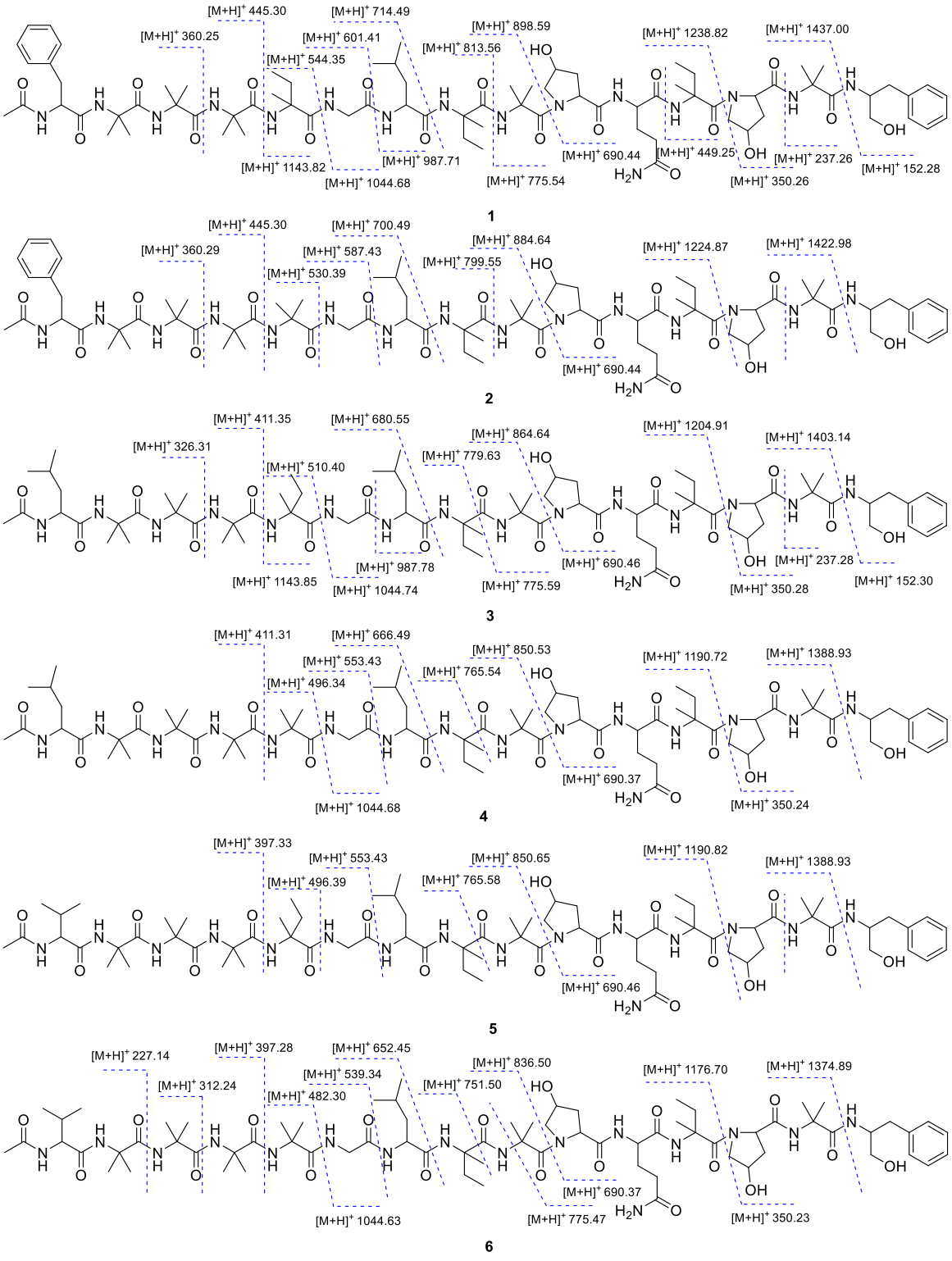

Figure 2. LC-MS/MS data for emerimicins V−X (**1**−**6**).

Aib^2-Aib^3-Aib^4-D-Iva^5-Gly^6-L-Leu^7-D-Iva^8-Aib^9-*trans*-L-Hyp^{10}-L-Gln^{11}-D-Iva^{12}-*trans*-L-Hyp^{13}-Aib^{14}-L-Pheol^{15} for **3**, *N*-Ac-L-Leu^1-Aib^2-Aib^3-Aib^4-Aib^5-Gly^6- L-Leu^7-D-Iva^8-Aib^9-*trans*-L-Hyp^{10}-L-Gln^{11}-D-Iva^{12}-*trans*-L-Hyp^{13}-Aib^{14}-L-Pheol^{15} for **4**, *N*-Ac-L-Val^1-Aib^2-Aib^3-Aib^4-D-Iva^5-Gly^6-L-Leu^7-D-Iva^8-Aib^9-*trans*-L-Hyp^{10}-L-Gln^{11}-D-Iva^{12}-*trans*-L-Hyp^{13}-Aib^{14}-L-Pheol^{15} for **5**, and *N*-Ac-L-Val^1-Aib^2-Aib^3-Aib^4-Aib^5-Gly^6-L-Leu^7-D-Iva^8-Aib^9-*trans*-L-Hyp^{10}-L-Gln^{11}-D-Iva^{12}-*trans*-L-Hyp^{13}-Aib^{14}-L-Pheol^{15} for **6**.

Emerimicins V−X are *N*-acetylated pentadecapeptide peptaibols and biosynthesized in an assembly line-like fashion by a large multimodular thiotemplated PKS-NRPS. This megasynthetase acts as a biosynthetic template in which the catalytic domains embedded in the enzyme dictate the number and type of building blocks that are to be incorporated into the final product, as well as any tailoring modifications. With polyketide biosynthesis, the general building blocks arise from

https://dx.doi.org/10.1021/acs.jnatprod.0c01186
J. Nat. Prod. 2021, 84, 1113−1126

Table 2. NMR Spectroscopic Data for Emerimicin VII (3) and Emerimicin VIII (4) in DMSO-d_6

3				4			
unit	position	δ_C	δ_H (J in Hz)	unit	position	δ_C	δ_H (J in Hz)
Ac	1	170.9 C		Ac	1	170.9 C	
	2	22.7 C	1.86, s		2	22.7 C	1.86, s
Leu[1]	1[a]	174.2 C		Leu[1]	1[a]	172.6 C	
	2	52.8 CH	4.09, m		2[b]	52.8 CH	4.09, m
	3	40.0 CH_2	1.46, m		3	40.0 CH_2	1.46, m
	4[b]	24.6 CH	1.68, m		4[c]	24.6 CH	1.64, m
	5[c]	22.2 CH_3	0.87, d (6.7)		5[d]	23.2 CH_3	0.92, d (6.8)
	6[d]	23.1 CH_3	0.92, d (6.6)		6[e]	22.1 CH_3	0.87, d (6.6)
	NH		8.16, d (5.7)		NH		8.17, d (5.6)
Aib[2]	1	176.6 C		Aib[2]	1[f]	175.7 C	
	2[e]	56.3 C			2[g]	56.4 C	
	3	25.6 CH_3	1.35, s		3[h]	25.1 CH_3	1.29, s
	4	25.3 CH_3	1.38, s		4[i]	23.9 CH_3	1.32, s
	NH		8.64, s		NH		8.67, s
Aib[3]	1[f]	176.1 C		Aib[3]	1[f]	175.6 C	
	2[e]	56.3 C			2[g]	56.3 C	
	3	25.0 CH_3	1.30, s		3[c]	24.6 CH_3	1.33, s
	4[b]	24.6 CH_3	1.33, s		4	25.7 CH_3	1.33, s
	NH		7.57, s		NH		7.61, s
Aib[4]	1	173.6 C		Aib[4]	1[j]	176.2 C	
	2[e]	56.6 C			2[g]	56.3 C	
	3[b]	24.6 CH_3	1.33, s		3[c]	24.3 CH_3	1.35, s
	4[b]	24.4 CH_3	1.34, s		4	26.2 CH_3	1.36, s
	NH		7.72, s		NH		7.71, s
Iva[5]	1[g]	175.6 C		Aib[5]	1	176.6 C	
	2	59.5 C			2[g]	56.3 C	
	3[h]	28.5 CH_2	2.13, m; 1.71, m		3[h]	25.1 CH_2	1.37, s
	4[i]	7.9 CH_3	0.79, t (7.4)		4	24.9 CH_3	1.38, s
	5	21.8 CH_3	1.35, s		NH		7.57, s
	NH		7.46, s				
Gly[6]	1[f]	176.0 C		Gly[6]	1[j]	176.2 C	
	2	43.9 CH_2	3.65, overlap;		2	44.0 CH_2	3.64, m;
			3.77, m, overlap				3.75, m overlap
	NH		7.95, t (5.8)		NH		8.00, t (5.5)
Leu[7]	1	172.6 C		Leu[7]	1[a]	172.3 C	
	2	53.6 CH	4.02, m		2	53.7 CH	4.02, m
	3	39.8 CH_2	1.54, m; 1.69, m		3	39.9 CH_2	1.53, m; 1.69, m
	4[b]	24.6 CH	1.68, m		4[c]	24.6 CH	1.67, m
	5[c]	22.0 CH_3	0.84, d (6.0)		5[e]	22.0 CH_3	0.85, d (7.6)
	6[d]	23.2 CH_3	0.90, d (6.3)		6[d]	23.1 CH_3	0.91, d (6.2)
	NH		7.74, overlap		NH		7.75, d (5.7)
Iva[8]	1[g]	175.5 C		Iva[8]	1[k]	174.3 C	
	2	59.9 C			2	59.9 C	
	3[h]	28.2 CH_2	2.20, m; 1.72, m		3	28.5 CH_2	2.14, m; 1.74, m
	4[i]	7.8 CH_3	0.74, t (6.7)		4	7.7 CH_3	0.72, t (7.5)
	5	22.4 CH_3	1.28, s		5	22.5 CH_3	1.28, s
	NH		7.38, s		NH		7.37, s
Aib[9]	1[a]	174.0 C		Aib[9]	1[k]	174.2 C	
	2[e]	56.7 C			2[g]	56.7 C	
	3	26.3 CH_3	1.36, s		3	25.6 CH_3	1.41, s
	4	23.6 CH_3	1.48, s		4	23.6 CH_3	1.48, s
	NH		7.56, s		NH		7.59, s
Hyp[10]	1	172.2 C		Hyp[10]	1[a]	172.4 C	
	2	61.6 CH	4.37, t (8.8)		2	61.5 CH	4.38, t (8.8)
	3	37.3 CH_2	1.78, m; 2.16, m		3	37.2 CH_2	1.77, m; 2.16, m
	4	69.5 CH	4.28, m		4[l]	69.5 CH	4.29, brs
	5[e]	56.7 CH_2	3.50, m; 3.74, m		5[g]	56.7 CH_2	3.51, m; 3.73, m
Gln[11]	1[f]	176.1 C		Gln[11]	1	173.6 C	
	2	53.0 CH	4.10, m		2[b]	52.8 CH	4.11, m

https://dx.doi.org/10.1021/acs.jnatprod.0c01186
J. Nat. Prod. 2021, 84, 1113−1126

Table 2. continued

	3				4		
unit	position	δ_C	δ_H (J in Hz)	unit	position	δ_C	δ_H (J in Hz)
	3	27.2 CH_2	1.88, overlap; 2.15, m		3	27.2 CH_2	1.88, overlap; 2.15, m
	4	32.0 CH_2	2.13, m		4	32.0 CH_2	2.12, m
	5	172.4 C			5	171.2 C	
	NH		7.87, d (8.5)		NH		7.89, d (8.9)
Iva[12]	1	171.2 C		Iva[12]	1[k]	174.0 C	
	2	58.7 C			2	58.7 C	
	3[h]	28.2 CH_2	2.21, m; 1.73, m		3	27.9 CH_2	2.22, m; 1.68, m
	4	7.4 CH_3	0.71, t (6.6)		4	7.4 CH_3	0.72, t (7.5)
	5	20.3 CH_3	1.40, s		5	20.3 CH_3	1.40, s
	NH		7.51, s		NH		7.48, s
Hyp[13]	1	171.9 C		Hyp[13]	1	172.0 C	
	2	62.3 CH	4.19, t (8.9)		2	62.4 CH	4.20, t (8.8)
	3[j]	37.0 CH_2	1.67,m; 2.10, m		3[m]	37.0 CH_2	1.66, m; 2.09, m
	4	68.5 CH	4.22, m		4[l]	69.4 CH	4.22, brs
	5	57.3 CH_2	3.65, m; 3.39, m		5	57.3 CH_2	3.65, dd (5.3, 18.3); 3.39, m
Aib[14]	1[a]	174.2 C		Aib[14]	1[k]	174.0 C	
	2[e]	56.5 C			2[g]	56.5 C	
	3	27.3 CH_3	1.15, s		3	27.3 CH_3	1.16, s
	4	23.9 CH_3	1.32, s		4[i]	23.9 CH_3	1.31, s
	NH		7.50, s		NH		7.51, s
Pheol[15]	1	63.8 CH	3.31, dd (7.3, 11.6); 3.39, overlap	Pheol[15]	1	63.8 CH	3.32, dd (6.5, 10.8); 3.38, overlap
	2	52.9 CH	3.88, m		2	52.9 CH	3.88, m
	3[j]	37.0 CH_2	2.54, overlap; 2.93, dd (13.7, 4.3)		3[m]	37.0 CH_2	2.53, overlap; 2.93, dd (13.9, 4.1)
	4	139.7 C			4	139.7 C	
	5/5′	129.5 CH	7.18, m		5/5′	129.5 CH	7.18, m overlap
	6/6′	128.3 CH	7.20, m		6/6′	128.3 CH	7.20, m overlap
	7	126.2 CH	7.12, m		7	126.2 CH	7.11, t (6.0)
	NH		6.97, d (8.8)		NH		6.98, d (9.1)

[a−m]The carbon chemical shifts are interchangeable, respectively.

simple acyl-Coenzyme A precursors, whereas in NRPS biosynthesis, proteinogenic and nonproteinogenic amino acids can be incorporated into the growing peptide chain. In modular NRPS systems, a typical module consists of condensation, adenylation, and thiolation domains. Adenylation (A) domains select and activate aminoacyl substrates, which then get loaded onto the phosphopantetheine prosthetic group of a thiolation (T) domain. The thiolation domain can then deliver the aminoacyl substrate to the condensation (C) domain, where it is coupled with the upstream nascent peptide. Additional tailoring domains within a module that further functionalize a building block include epimerization (E), formylation, cyclization, oxidation, and reduction domains. Initial scanning of the 38 Mbp genome of *A. tubakii* revealed the presence of 44 biosynthetic clusters, with two appearing to be peptaibol-related. The two putative peptaibol clusters contained A domains with selectivity for the α,α-dialkylated α-amino acid Aib, an N-terminal acetyl transferase domain, and a C-terminal reductive offloading domain. However, only one cluster, the 60 kbp *eme* biosynthetic cluster, contained the sufficient number of modules required for assembling **1**−**6**. The *eme* cluster was annotated to encode three open reading frames (Figure 3, Table S8), including the 56 kb hybrid PKS-NRPS *eme*B. In addition to *eme*B, the *eme* gene cluster also encodes a 2-oxoglutarate Fe(II)-dependent oxygenase (*eme*C) that would oxidize the two proline residues found in all six emerimicins to 4-hydroxy-proline. A closer inspection of the 16 modules in EmeB revealed the presence of 15 A domains, which corroborate with the 15-amino-acid-containing emerimicins. The loading module of EmeB also harbors an acyltransferase (AT) domain that would be responsible for incorporating an acetate unit onto the N-terminus of the pentadecapeptides, and the domain architecture of the loading module is similar to other peptaibol biosynthetic clusters associated with *N*-acetylated peptides.[17] Finally, EmeB ends with a reductase domain that would release the pentadecapeptide from the enzyme and reduce the C-terminal L-Phe to L-phenylalaninol (L-Pheol).

Using detailed bioinformatic analysis and latent semantic indexing,[18] the substrate specificities of the 15 A domains from EmeB were predicted (Table 4 and Figure S77) and shown to be in agreement with what was determined through NMR, LC-MS/MS, and Marfey's method. Interestingly, while D-Iva was detected in **1**−**6** via spectroscopic and chemical methods, modules 8 and 12 did not contain an E domain that is known to catalyze the L- to D-epimerization of amino acids in NRPS biosynthesis. This suggests that the A domains in modules 8 and 12 select and activate the nonproteinogenic building block D-Iva and load it onto their respective T domains. This finding, in addition to latent semantic indexing being able to predict α,α-dialkylyated amino acid substrate specificity for modules 2, 3, 4, 5, 8, 9, 12, and 14, further supports that some fungi are capable of producing α,α-dialkylyated amino acids and the

https://dx.doi.org/10.1021/acs.jnatprod.0c01186
J. Nat. Prod. 2021, 84, 1113−1126

Table 3. NMR Spectroscopic Data for Emerimicin IX (5) and Emerimicin X (6) in DMSO-d_6

5				6			
unit	position	δ_C	δ_H (J in Hz)	unit	position	δ_C	δ_H (J in Hz)
Ac	1	171.1 C		Ac	1[a]	171.2 C	
	2	22.7 C	1.89, s		2	22.7 C	1.89, s
Val[1]	1	173.1 C		Val[1]	1	176.6 C	
	2	60.3 CH	3.82, m		2	60.3 CH	3.82, m
	3	29.5 CH	1.93, m		3	29.5 CH	1.93, m
	4	19.6 CH_3	0.95, d (6.6)		4	19.6 CH_3	0.95, d (6.9)
	5	19.4 CH_3	0.81, d (6.3)		5	19.4 CH_3	0.91, overlap
	NH		8.11, d (5.8)		NH		8.10, d (5.9)
Aib[2]	1[a]	175.4 C		Aib[2]	1[b]	175.5 C	
	2[b]	56.4 C			2[c]	56.4 C	
	3	21.7 CH_3	1.35, s		3	25.5 CH_3	1.41, s
	4[c]	24.1 CH_3	1.36, s		4	25.2 CH_3	1.28, s
	NH		8.65, s		NH		8.65, s
Aib[3]	1[a]	175.6 C		Aib[3]	1[d]	176.2 C	
	2[b]	56.4 C			2[c]	56.4 C	
	3[c]	24.4 CH_3	1.34, s		3	24.4 CH_3	1.34, s
	4	25.1 CH_3	1.38, s		4	24.0 CH_3	1.37, s
	NH		7.53, s		NH		7.54, overlap
Aib[4]	1[d]	172.4 C		Aib[4]	1[b]	175.6 C	
	2[b]	56.7 C			2[c]	56.3 C	
	3[e]	25.6 CH_3	1.36, s		3[e]	25.0 CH_3	1.37, s
	4[e]	25.8 CH_3	1.35, s		4[e]	25.0 CH_3	1.37, s
	NH		7.77, s		NH		7.73, s
Iva[5]	1	176.6 C		Aib[5]	1[d]	176.1 C	
	2	59.5 C			2[c]	56.3 C	
	3[f]	28.5 CH_2	2.14, m; 1.72, m		3[f]	26.0 CH_2	1.34, s
	4	8.0 CH_3	0.80, t (7.4)		4	25.6 CH_3	1.36, s
	5	25.3 CH_3	1.29, s		NH		7.54, overlap
	NH		7.48, s				
Gly[6]	1[g]	176.0 C		Gly[6]	1[a]	171.2 C	
	2	43.8 CH_2	3.65, m, overlap; 3.77, m overlap		2	43.9 CH_2	3.64, m, overlap; 3.76, m overlap
	NH		7.95, t (4.7)		NH		7.99, t (5.9)
Leu[7]	1[h]	174.3 C		Leu[7]	1[g]	174.2 C	
	2	53.6 CH	4.03, m		2	53.7 CH	4.02, m
	3	39.9 CH_2	1.54, m; 1.69, m		3	39.9 CH_2	1.53, m; 1.69, m
	4	24.6 CH	1.69, m		4[f]	26.0 CH	1.64, m
	5	22.1 CH_3	0.85, d (6.0)		5	22.1 CH_3	0.85, d (6.0)
	6	23.1 CH_3	0.91, d (6.3)		6	23.1 CH_3	0.91, overlap
	NH		7.73, d (5.6)		NH		7.74, overlap
Iva[8]	1[h]	174.2 C		Iva[8]	1	173.6 C	
	2	59.9 C			2	59.9 C	
	3[f]	28.3 CH_2	2.20, m; 1.72, m		3	28.5 CH_2	2.14, m; 1.75, m
	4	7.8 CH_3	0.74, t (7.2)		4	7.8 CH_3	0.72, t (7.2)
	5	22.3 CH_3	1.28, s		5	22.5 CH_3	1.27, s
	NH		7.42, s		NH		7.38, s
Aib[9]	1[h]	174.0 C		Aib[9]	1[g]	174.0 C	
	2[b]	56.7 C			2[c]	56.7 C	
	3	26.3 CH_3	1.35, s		3	26.2 CH_3	1.36, s
	4	23.6 CH_3	1.48, s		4	23.6 CH_3	1.48, s
	NH		7.60, s		NH		7.58, s
Hyp[10]	1[d]	172.2 C		Hyp[10]	1[h]	172.3 C	
	2	61.6 CH	4.38, t (8.9)		2	61.5 CH	4.37, t (8.6)
	3	37.3 CH_2	1.78, m; 2.16, m		3	37.2 CH_2	1.77, m; 2.16, m
	4	69.5 CH	4.28, m		4[i]	69.5 CH	4.29, m
	5[b]	56.5 CH_2	3.50, m; 3.74, m		5[c]	56.7 CH_2	3.51, m; 3.73, m
Gln[11]	1[g]	176.0 C		Gln[11]	1	173.1 C	
	2	53.0 CH	4.11, m		2	53.0 CH	4.11, m
	3	27.2 CH_2	1.89, overlap; 2.15, m		3	27.2 CH_2	1.89, overlap; 2.16, m

https://dx.doi.org/10.1021/acs.jnatprod.0c01186
J. Nat. Prod. 2021, 84, 1113−1126

Table 3. continued

5				6			
unit	position	δ_C	δ_H (J in Hz)	unit	position	δ_C	δ_H (J in Hz)
	4	32.0 CH_2	2.13, m		4	32.0 CH_2	2.12, m
	5	173.6 C			5	172.6 C	
	NH		7.87, d (8.5)		NH		7.88, d (8.8)
Iva[12]	1	171.9 C		Iva[12]	1[h]	172.4C	
	2	58.7 C			2	58.7 C	
	3[f]	28.3 CH_2	2.20, m; 1.70, m		3	28.0 CH_2	2.22, m; 1.69, m
	4	7.4 CH_3	0.72, t (7.4)		4	7.4 CH_3	0.72, t (7.2)
	5	20.3 CH_3	1.40, s		5	20.3 CH_3	1.38, s
	NH		7.47, s		NH		7.47, s
Hyp[13]	1[d]	172.6 C		Hyp[13]	1	171.9 C	
	2	62.3 CH	4.20, t (8.9)		2	62.4 CH	4.20, t (10.4)
	3[i]	37.0 CH_2	1.67,m; 2.10, m		3[j]	37.0 CH_2	1.68, m; 2.11, m
	4	68.5 CH	4.22, m		4[i]	69.4 CH	4.22, m
	5	57.3 CH_2	3.65, m; 3.39, m		5	57.3 CH_2	3.64, m; 3.39, m
Aib[14]	1[h]	174.2 C		Aib[14]	1[g]	174.3 C	
	2[b]	56.5 C			2[c]	56.5 C	
	3	27.3 CH_3	1.16, s		3	27.4 CH_3	1.16, s
	4[c]	23.9 CH_3	1.32, s		4	23.9 CH_3	1.31, s
	NH		7.50, s		NH		7.50, s
Pheol[15]	1	63.8 CH	3.31, dd (7.3, 11.0); 3.39, overlap	Pheol[15]	1	63.8 CH	3.31, dd (6.6, 10.5); 3.39, overlap
	2	52.9 CH	3.88, m		2	52.9 CH	3.88, m
	3	37.0 CH_2	2.54, overlap; 2.94, dd (14.7, 4.1)		3[j]	37.0 CH_2	2.54, overlap; 2.94, dd (13.8, 4.4)
	4	139.7 C			4	139.7 C	
	5/5′	129.5 CH	7.18, m overlap		5/5′	129.5 CH	7.18, m overlap
	6/6′	128.3 CH	7.20, m overlap		6/6′	128.3 CH	7.20, m overlap
	7	126.2 CH	7.12, t (6.9)		7	126.2 CH	7.11, t (6.0)
	NH		6.97, d (9.2)		NH		6.98, dd (8.7, 9.2)

[a−j]The carbon chemical shifts are interchangeable, respectively.

nonproteinogenic amino acids are not formed by post-NRPS tailoring reactions.[5,7]

The antibacterial activity of compounds **1**−**6** and helvolic acid was evaluated against *E. faecalis*, vancomycin-resistant *E. faecium* (VRE), methicillin-resistant *S. aureus* (MRSA), and *Pseudomonas aeruginosa*. While the emerimicins did not display activity against *P. aeruginosa*, compound **1** exhibited modest antibacterial activity against *E. faecalis*, VRE, and MRSA with MIC values of 64, 64, and 32 μg/mL, respectively, and compound **2** showed activity against MRSA with a MIC value of 64 μg/mL (Table 5). Helvolic acid possessed potent activity against the bacterial pathogens suggesting it was responsible for the antimicrobial activity initially observed in the crude extract of *A. tubakii*.[13] Interestingly, while **1** and **2** displayed modest or weak antibacterial activity, compounds **3**−**6** did not exhibit any notable activity toward *E. faecalis*, VRE, or MRSA. A structure comparison of the emerimicins show that while the amino acid sequences of **1**, **3**, and **5** are nearly identical, the swapping of the N-terminal Phe residue found in **1** with either Leu or Val, dramatically decreases the antimicrobial activity. As many peptaibols, especially the 20-residue alamethicins,[19] are known cytotoxic agents, with many possessing cancer cell selectivity,[20] the toxicity profiles of **1**−**6** were assessed using a zebrafish embryotoxicity assay. While **1** and **2** were the most active in the antimicrobial screen, both compounds displayed significant embryotoxicity at 33 μg/mL (Figure S78). However, while **3**−**6** did not possess any antimicrobial activity, compounds **3** and **4** demonstrated significant embryotoxicity at 100 μg/mL, whereas compunds **5** and **6** had a mean embryo survival rate of 75% and 70%, respectively, at 100 μg/mL. These data further demonstrate that the toxicity profiles are also affected by the exchange of Phe[1] with Leu or Val.

In summary, while hundreds of peptaibols have been described in the literature,[21−23] 15 amino acid residue-containing peptaibols are relatively rare, with <25 currently reported (Table S1). Herein, we identified six new 15-residue peptaibols, emerimicins V−X, produced by the filamentous fungus *A. tubakii*. The amino acid composition of the six emerimicins, along with the absolute configuration of all residues, was determined through a combination of 1D and 2D NMR experiments, LC-MS/MS, and advanced Marfey's method. Structurally, the amino acid sequences of emerimicins V−X are similar to those of emerimicin IV and bergofungins A−C.[14,24,25] However, the emerimicins isolated from *A. tubakii* W. Gams display a higher proportion of nonproteinogenic amino acid residues. Additionally, variability among emerimicins V−X was also observed, most notably at residue 1. While emerimicins V and VI both contain L-Phe, emerimicins VII and VIII contain L-Leu, whereas emerimicins IX and X contain L-Val. The difference in residues observed in emerimicins V−X highlights the flexibility of the adenylation domain in the first module for selecting and activating a variety of amino acid substrates. Interestingly, of the reported 15-amino-acid-containing peptaibols, Aib, Phe, Val, and Try are the most common residues located at the N-terminus. Leu is rarely found as a starting residue in peptaibols, but has been

https://dx.doi.org/10.1021/acs.jnatprod.0c01186
J. Nat. Prod. 2021, 84, 1113−1126

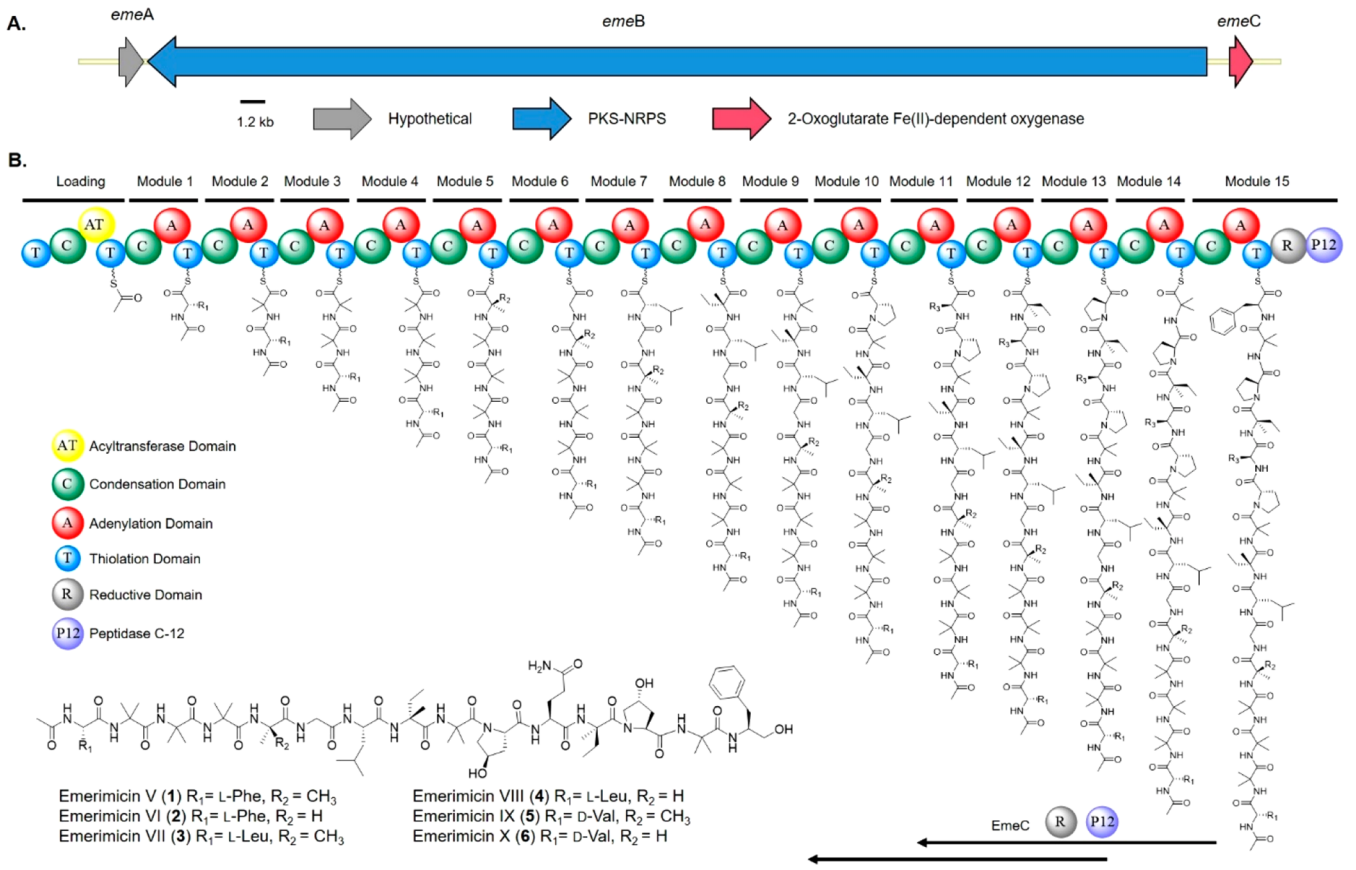

Figure 3. Proposed emerimicin biosynthesis. (A) Organization of the *eme* gene cluster (GenBank accession number MT050462). (B) Domain organization of the 16-module PKS-NRPS EmeB and formation of the emerimicins V–X (**1**–**6**). In panel B, starting with module 11, R_3 = L-Gln. The arrows represent open reading frames and point in the direction of transcription.

Table 4. Predicted and Observed Amino Acid Residues in 1–6[a]

EmeB module	predicted amino acid	LSI score	residues in 1 and 2	residues in 3 and 4	residues in 5 and 6
1	Glu	0.434	L-Phe	L-Leu	L-Val
	Val	0.363			
	Leu	0.355			
2	Iva	0.971	Aib	Aib	Aib
3	Iva	0.971	Aib	Aib	Aib
4	Iva	0.971	Aib	Aib	Aib
5	Iva	0.527	**1** D-Iva	**3** D-Iva	**5** D-Iva
			2 Aib	**4** Aib	**6** Aib
6	Gly	0.558	Gly	Gly	Gly
7	Leu	0.624	L-Leu	L-Leu	L-Leu
8	Val	0.710	D-Iva	D-Iva	D-Iva
	Iva	0.493			
9	Iva	0.971	Aib	Aib	Aib
10	Lys	0.566	L-Pro	L-Pro	L-Pro
11	Gln	0.925	L-Gln	L-Gln	L-Gln
12	Iva	0.520	D-Iva	D-Iva	D-Iva
13	Ala	0.515	L-Pro	L-Pro	L-Pro
	Pro	0.361			
14	Iva	0.921	Aib	Aib	Aib
15	Phe	0.446	L-Phe	L-Phe	L-Phe

[a]Latent semantic indexing was used to calculate amino acid specificities for each A domain in EmeB.

reported in antiamoebins XV and XVI[26] and Leu[1]-zervamicin,[27] which are all 16-amino-acid-containing peptides. Therefore, emerimicin VII (**3**) and emerimicin VIII (**4**) represent the first reported pentadecapeptide peptaibols containing L-Leu at the N-terminus. A preliminary structure–activity relationship between emerimicins V–X also revealed that **1** and **2** displayed modest or weak antimicrobial activity compared to **3**–**6**. While **1** was the most active, it shares sequence similarities with **3** and **5**, with the only difference residing at residue 1. This change in biological activity has been observed with trichodermides A–E[28] and further emphasizes how activity can be changed dramatically by a single amino acid swap. Furthermore, the emerimicins were evaluated for their toxicity effects on zebrafish embryos. While **1** and **2** were the most active in the antimicrobial screen, both compounds, in addition to **3** and **4**, displayed significant embryotoxicity compared to **5** and **6**.

EXPERIMENTAL SECTION

General Experimental Procedures. Specific optical rotations were measured on a Jasco DIP-370 polarimeter at 20 °C, and UV spectra were recorded on a PerkinElmer Lambda2 UV/vis spectrometer. NMR spectra were recorded on Varian INOVA 500 and 600 NMR spectrometers with 3 mm Nalorac MDBG probes. All spectra were acquired in DMSO-d_6 and referenced to ^{1}H (2.49 ppm) or ^{13}C (39.5 ppm) in the deuterated solvent. High-resolution ESIMS was carried out on a Bruker Maxis II ETD Q-TOF instrument, and HPLC-MS/MS was recorded using a Micromass Q-TOF Micro mass spectrometer (Waters) in positive mode with an Agilent Eclipse XDB-C_{18} column (150 × 4.6 mm, 5 μm). Column chromatography was performed using 230–400 mesh silica gel (Natland International Corporation, USA).

https://dx.doi.org/10.1021/acs.jnatprod.0c01186
J. Nat. Prod. 2021, 84, 1113–1126

Table 5. MIC Values of 1−6 and Helvolic Acid

	MIC (μg/mL)							
	1	2	3	4	5	6	helvolic acid	gentamicin
Enterococcus faecalis	64	>100	>100	>100	>100	>100	16	8
vancomycin-resistant *Enterococcus faecium*	64	>100	>100	>100	>100	>100	8	4
methicillin-resistant *Staphylococcus aureus*	32	64	>100	>100	>100	>100	4	4
Pseudomonas aeruginosa	>100	>100	>100	>100	>100	>100	>100	2

Identification and Genome Sequencing of *A. tubakii*. *A. tubakii* was isolated from soil collected on the University of Utah campus, UT, USA, and a voucher specimen is deposited in our laboratory collection. Partial ITS sequencing (GenBank accession number MT053262) initially identified the strain as an *Acremonium* species. For a more reliable identification, full-length ITS sequences for the isolate that we initially called *Acremonium* sp. "PF" were extracted from the whole genome assembly with BLASTn using *Acremonium* sp. (INSD accession KP131516) as a query. The resulting sequence was then used as a query to identify and combine with the top 100 best BLAST hits in the UNITE+INSD v.8.2 fungi data set,[29] which consists of 714 329 curated fungal ITS sequences. Fast Fourier transform (MAFFT) version 7 was used to create the multiple sequence alignment with the L-INS-i algorithm, and phylogenetic inference was generated using a maximum likelihood implemented in IQ-TREE,[30] using ModelFinder[31] to first identify the best-fit substitution model and then infer the best ML tree (option −m TEST). Branch support was calculated using ultrafast bootstrapping (1000 replicates)[32,33] and the SH-like approximate likelihood ratio test (1000 replicates).[34] The resulting tree (Figure S79) is midpoint-rooted, and terminal labels include INSD accession number, taxon identification, and UNITE species hypothesis numbers.

For extraction of gDNA, *A. tubakii* was cultured in 100 mL of GYEC media (15 g/L glucose, 3 g/L yeast extract, 5 g/L peptone) at 25 °C for 96 h at 250 rpm. The mycelia were harvested by centrifugation, lyophilized overnight, and ground to a fine powder. A slurry was created using 1 g of dry weight per 12 mL of lysis buffer (50 mM Tris, 50 mM EDTA, 2% SDS, pH 8.0) and incubated in a 65 °C water bath for 30 min. The mixture was then centrifuged at 21000*g* for 15 min at room temperature, and the supernatant was extracted with an equal volume of phenol−chloroform−isoamyl alcohol (25:24:1) pH 8.0. Samples were centrifuged as described above, and gDNA was isolated from the aqueous layer using ethanol−ammonium acetate precipitation. The isolated gDNA was resuspended in 10 mM Tris-HCl pH 8.0, treated with RNase A (0.5 mg/mL) by incubating at 50 °C for 30 min, and then stored at 4 °C. The genome of *A. tubakii* was sequenced at the High-Throughput Genomics Core at the Huntsman Cancer Institute at the University of Utah. A 250 bp PCR-free DNA library was constructed and sequenced using Illumina HiSeq (125 cycle paired-end), resulting in >250× coverage. Genome assembly was performed using SPAdes version 3.13.0.[35] Assembly of the 38 Mbp genome resulted in 223 scaffolds with an N_{50} of 2 297 316 bp. The sequence data were used to create a local BLAST database using Blast+ software,[36] and, using the tblastn commands and antiSMASH analysis,[37−39] 22 NRPS-containing biosynthetic clusters were identified, including the *eme* cluster encoding a 16-module PKS−NRPS hybrid enzyme. The amino acid specificities of the 15 adenylation domains in *Eme*B were analyzed using latent semantic indexing[18] (Table 4 and Figure S77).

Fermentation, Extraction, and Isolation of 1−6. *A. tubakii* was cultured in 100 mL of potato dextrose broth (Difco) in a 500 mL Erlenmeyer flask for 9 days at 28 °C with constant shaking at 160 rpm. The mycelium and media were extracted with an equal volume of ethyl acetate containing 1% acetic acid, dried over anhydrous $MgSO_4$, and concentrated *in vacuo*. The crude extract was resuspended in DMSO and analyzed for activity against several bacterial pathogens, including *E. faecalis*, vancomycin-resistant *E. faecium*, methicillin-resistant *S. aureus*, and *P. aeruginosa*. The crude extract showed potent antibacterial activity against methicillin-resistant *S. aureus, E. faecalis*, and vancomycin-resistant *E. faecium*.

To isolate the active molecule(s), *A. tubakii* was cultured for 9 days in eight 2.8 L Fernbach flasks, each containing 1 L potato dextrose broth (Difco), at 28 °C with constant shaking at 160 rpm. After the 9-day fermentation, the cultures were combined and centrifuged at 3000 rpm at room temperature for 20 min, and the supernatant was incubated with HP-20 resin (20 g/L) under constant shaking at 120 rpm for 2 h. The resin was then filtered through Miracloth, washed with water three times (200 mL each time) to remove salts, and extracted three times with acetone (300 mL each time) to yield the crude extract. The combined acetone crude extract was concentrated *in vacuo* and partitioned with ethyl acetate and water to yield the ethyl acetate crude extract (2.6 g). Using normal silica gel chromatography, the extract was fractionated into seven fractions using different concentrations of hexane, ethyl acetate, and methanol. Fraction 4 eluted with a mixture of ethyl acetate−methanol (95%:5%) and was subjected to further purification via semipreparative HPLC (78:22 MeOH−H_2O with 0.1% TFA, 3 mL/min) using an ODS column (Luna, C_{18}(2), LC column 10 × 250 mm, 5 μm) to yield helvolic acid (8.0 mg, t_R = 16.1 min). Fraction 6 eluted with a mixture of ethyl acetate−methanol (70%:30%) and was further purified by semi-preparative HPLC (78:22 MeOH−H_2O with 0.1% TFA, 3 mL/min) using the same ODS column as fraction 4 to yield compounds **1** (3.1 mg), a mixture of **2** and **5**, **3** (7.2 mg), **4** (9.0 mg), and **6** (5.7 mg). The mixture of **2** and **5** was subjected to further purification by HPLC (55:45 MeCN−H_2O with 0.1% TFA, 3 mL/min) to afford pure compounds **2** (2.4 mg) and **5** (3.4 mg).

*Emerimicin V (**1**).* White powder; $[\alpha]^{20}_D$ +2.0 (*c* 0.1, $CHCl_3$); UV, Figure S1; ^1H and ^{13}C NMR data, Table 1 and Supporting Information; HRESIMS *m*/*z* 794.4609 $[M + 2H]^{2+}$ (calcd for $C_{78}H_{122}N_{16}O_{19}$, 794.4609) (Figure S19).

*Emerimicin VI (**2**).* White powder; $[\alpha]^{20}_D$ +1.4 (*c* 0.1, $CHCl_3$); UV, Figure S1; ^1H and ^{13}C NMR data, Table 1 and Supporting Information; HRESIMS *m*/*z* 787.4531 $[M + 2H]^{2+}$ (calcd for $C_{77}H_{120}N_{16}O_{19}$, 787.4531) (Figure S29).

*Emerimicin VII (**3**).* White powder; $[\alpha]^{20}_D$ +1.3 (*c* 0.1, $CHCl_3$); UV, Figure S1; ^1H and ^{13}C NMR data, Table 2 and Supporting Information; HRESIMS *m*/*z* 777.4653 $[M + 2H]^{2+}$ (calcd for $C_{75}H_{124}N_{16}O_{19}$, 777.4687) (Figure S41).

*Emerimicin VIII (**4**).* White powder; $[\alpha]^{20}_D$ +1.7 (*c* 0.1, $CHCl_3$); UV, Figure S1; ^1H and ^{13}C NMR data, Table 2 and Supporting Information; HRESIMS *m*/*z* 770.4578 $[M + 2H]^{2+}$ (calcd for $C_{74}H_{122}N_{16}O_{19}$, 770.4609) (Figure S55).

*Emerimicin IX (**5**).* White powder; $[\alpha]^{20}_D$ +2.0 (*c* 0.1, $CHCl_3$); UV, Figure S1; ^1H and ^{13}C NMR data, Table 3 and Supporting Information; HRESIMS *m*/*z* 770.4576 $[M + 2H]^{2+}$ (calcd for $C_{74}H_{122}N_{16}O_{19}$, 770.4609) (Figure S64).

*Emerimicin X (**6**).* White powder; $[\alpha]^{20}_D$ −3.0 (*c* 0.1, $CHCl_3$); UV, Figure S1; ^1H and ^{13}C NMR data, Table 3 and Supporting Information; HRESIMS *m*/*z* 763.4498 $[M + 2H]^{2+}$ (calcd for $C_{73}H_{120}N_{16}O_{19}$, 763.4531) (Figure S75).

Advanced Marfey's Analysis. Each peptide (~0.2 mg) was dissolved in 6 N HCl (500 μL) and heated in a glass ampule for 12 h at 110 °C. The hydrolysate was evaporated to dryness *in vacuo* and redissolved in 100 μL of H_2O. The solution was split into two equal fractions, and to each fraction were added 20 μL of 1 N $NaHCO_3$ and 100 μL of L-FDLA (1% solution in acetone). The mixture was heated for 50 min at 40 °C, quenched with 20 μL of 1 N HCl, and dried *in vacuo*. The residue was dissolved in 1:1 CH_3CN−H_2O and analyzed

https://dx.doi.org/10.1021/acs.jnatprod.0c01186
J. Nat. Prod. 2021, 84, 1113−1126

by LC-MS. Separation of the amino acids was carried out using an Agilent Eclipse XDB-C_{18} column (5 μm, 4.6 × 150 mm) at a flow rate of 0.5 mL/min with a linear gradient of 5% to 100% CH_3CN with 0.1% formic acid over 45 min. All L-FDLA derivatives of D and L amino acid standards were purchased from Sigma-Aldrich and prepared as above. Absolute configurations of amino acids were determined by comparing the retention times of L-FDLA hydrolysate derivatives to the D,L- and L-FDLA amino acid standards, which were identified by MS. Retention times of the L-FDLA amino acid derivatives were 20.58 min (*trans*-4-OH-L-proline) and 20.67 min (*trans*-4-OH-D-proline), 27.64 min (L-Leu) and 31.59 min (D-Leu), 26.11 min (L-Val) and 29.64 min (D-Val), 27.06 min (L-Iva) and 28.47 min (D-Iva), 23.03 min (D-Glu-D-FDLA) and 23.61 min (D-Glu-L-FDLA), 28.58 min (L-Pheol) and 30.91 min (D-Pheol), and 27.89 min (L-Phe) and 30.62 min (D-Phe) (Figure S76).

Antibacterial Assays. Broth microdilution assays were used to screen **1**−**6** and helvolic acid for bioactivity, as well as the crude extract of *A. tubakii*. All assays were performed according to the Clinical & Laboratory Standards Institute (CLSI) guidelines. To prepare the inoculum for susceptibility testing, bacteria were streaked onto Muller Hinton agar (MHA) and incubated overnight at 37 °C. Individual colonies were then isolated and transferred to 5 mL of cation adjusted Mueller Hinton broth (CAMHB) and incubated at 37 °C for 2−6 h. The culture density was adjusted with CAMHB so that a concentration of 5 × 10^6 cfu/mL was achieved. The initial percent inhibition of the crude extract was evaluated using 100 μg/mL of crude extract dissolved in DMSO, and significant growth inhibition of methicillin-resistant *S. aureus* (ATCC 1556), *E. faecalis* (ATCC 19433), and vancomycin-resistant *E. faecium* (ATCC 51299) was observed. Emerimicins **1**−**6** and helvolic acid were then tested for their individual activity against *E. faecalis*, vancomycin-resistant *E. faecium*, methicillin-resistant *S. aureus*, and *P. aeruginosa* (ATCC 27853) using gentamicin as a positive control (64 μg/mL dissolved in water). Briefly, **1**−**6** and helvolic acid were dissolved in DMSO to generate 100 mM stock solutions. The stock solutions were then serially diluted with CAMHB to afford working concentrations of 200 to 2 μM. To a 96-well microtiter plate, 100 μL aliquots of the diluted compounds were added to 10 μL of density-adjusted microbial culture. The plates were incubated at 37 °C for 16−20 h. MIC values were determined by visual inspection and verified with an OD_{600} measurement using a BioTek Neo2 plate reader. The respective MIC values for **1**−**6**, as well as helvolic acid and gentamicin, are reported in Table 5.

Zebrafish Assay. Zebrafish embryos were obtained, and the animals were maintained according to standard fish husbandry protocols. Fertilized eggs were collected from group mating of TuAB zebrafish and stored in 1× E3 media (5 mM NaCl, 0.17 mM KCl, 0.33 mM $CaCl_2$, 0.33 mM $MgSO_4$) at 28 °C until 24 h postfertilization (hpf). At 24 hpf, groups of 5 embryos were distributed into the wells of flat-bottom 96-well plates filled with 400 μL of 1× E3 media. Compounds **1**−**6** were dissolved in DMSO to provide 100 mg/mL stock solutions. The stock solutions were serially diluted with DMSO to give concentrations of 10 mg/mL to 4.6 μg/mL. To each 400 μL well, 4 μL aliquots of each dilution for **1**, **2**, **3**, **4**, **5**, or **6** were added so that the final concentrations of compound being tested ranged from 100 to 0.046 μg/mL, and all wells contained no greater than 1% DMSO. The plates of embryos were then incubated at 28 °C for 48 h, after which the number of surviving embryos were counted. All zebrafish protocols were approved by the Institutional Animal Care and Use Committee at the University of Utah.

■ ASSOCIATED CONTENT

Supporting Information

The Supporting Information is available free of charge at https://pubs.acs.org/doi/10.1021/acs.jnatprod.0c01186.

Experimental details on NMR spectroscopic data, mass spectra, EmeB adenylation domain sequences, and hypocreales 28S phylogenetic tree (PDF)

■ AUTHOR INFORMATION

Corresponding Author

Jaclyn M. Winter − *Department of Medicinal Chemistry, University of Utah, Salt Lake City, Utah 84112, United States;* orcid.org/0000-0001-6273-5377; Phone: 801-585-7117; Email: jaclyn.winter@utah.edu; Fax: 801-585-6208

Authors

Guangwei Wu − *Department of Medicinal Chemistry, University of Utah, Salt Lake City, Utah 84112, United States*

Bryn T. M. Dentinger − *Natural History Museum of Utah & School of Biological Sciences, University of Utah, Salt Lake City, Utah 84108, United States*

Jason R. Nielson − *Department of Pharmacology and Toxicology, University of Utah, Salt Lake City, Utah 84112, United States*

Randall T. Peterson − *Department of Pharmacology and Toxicology, University of Utah, Salt Lake City, Utah 84112, United States;* orcid.org/0000-0003-0727-3469

Complete contact information is available at: https://pubs.acs.org/10.1021/acs.jnatprod.0c01186

Notes

The authors declare no competing financial interest.

■ ACKNOWLEDGMENTS

This work was supported by the Gordon and Betty Moore Foundation (GMBF7621) to J.M.W. We thank M. Landward (University of Utah) for performing antimicrobial activity screening, Dr. J. Skalicky (University of Utah) for helpful NMR discussions, and Ms. P. Fung from the mycology course (BIOL 5425) at the University of Utah for isolating the fungus for this study.

■ REFERENCES

(1) Sussmuth, R. D.; Mainz, A. *Angew. Chem., Int. Ed.* **2017**, *56*, 3770−3821.

(2) Szekeres, A.; Leitgeb, B.; Kredics, L.; Antal, Z.; Hatvani, L.; Manczinger, L.; Vagvolgyi, C. *Acta Microbiol. Immunol. Hung.* **2005**, *52*, 137−168.

(3) Daniel, J. F.; Filho, E. R. *Nat. Prod. Rep.* **2007**, *24*, 1128−1141.

(4) Degenkolb, T.; von Dohren, H.; Nielsen, K. F.; Samuels, G. J.; Bruckner, H. *Chem. Biodiversity* **2008**, *5*, 671−680.

(5) Bruckner, H.; Becker, D.; Gams, W.; Degenkolb, T. *Chem. Biodiversity* **2009**, *6*, 38−56.

(6) Degenkolb, T.; Bruckner, H. *Chem. Biodiversity* **2008**, *5*, 1817−1843.

(7) Raap, J.; Erkelens, K.; Ogrel, A.; Skladnev, D. A.; Bruckner, H. *J. Pept. Sci.* **2005**, *11*, 331−338.

(8) Degenkolb, T.; Kirschbaum, J.; Bruckner, H. *Chem. Biodiversity* **2007**, *4*, 1052−1067.

(9) Marik, T.; Tyagi, C.; Balazs, D.; Urban, P.; Szepesi, A.; Bakacsy, L.; Endre, G.; Rakk, D.; Szekeres, A.; Andersson, M. A.; Salonen, H.; Druzhinina, I. S.; Vagvolgyi, C.; Kredics, L. *Front. Microbiol.* **2019**, *10*, 1434.

(10) Du, L.; Risinger, A. L.; Mitchell, C. A.; You, J.; Stamps, B. W.; Pan, N.; King, J. B.; Bopassa, J. C.; Judge, S. I. V.; Yang, Z.; Stevenson, B. S.; Cichewicz, R. H. *Proc. Natl. Acad. Sci. U. S. A.* **2017**, *114*, E8957−E8966.

(11) Whitmore, L.; Wallace, B. A. *Eur. Biophys. J.* **2004**, *33*, 233−237.

(12) Lv, J. M.; Hu, D.; Gao, H.; Kushiro, T.; Awakawa, T.; Chen, G. D.; Wang, C. X.; Abe, I.; Yao, X. S. *Nat. Commun.* **2017**, *8*, 1644.

(13) Ratnaweera, P. B.; Williams, D. E.; de Silva, E. D.; Wijesundera, R. L.; Dalisay, D. S.; Andersen, R. J. *Mycology* **2014**, *5*, 23−28.
(14) Inostroza, A.; Lara, L.; Paz, C.; Perez, A.; Galleguillos, F.; Hernandez, V.; Becerra, J.; Gonzalez-Rocha, G.; Silva, M. *Nat. Prod. Res.* **2018**, *32*, 1361−1364.
(15) Fujii, K.; Ikai, Y.; Mayumi, T.; Oka, H.; Suzuki, M.; Harada, K. *Anal. Chem.* **1997**, *69*, 3346−3352.
(16) Fujii, K.; Ikai, Y.; Oka, H.; Suzuki, M.; Harada, K. *Anal. Chem.* **1997**, *69* (24), 5146−5151.
(17) Dewapriya, P.; Khalil, Z. G.; Prasad, P.; Salim, A. A.; Cruz-Morales, P.; Marcellin, E.; Capon, R. J. *Front. Chem.* **2018**, *6*, 394.
(18) Baranasic, D.; Zucko, J.; Diminic, J.; Gacesa, R.; Long, P. F.; Cullum, J.; Hranueli, D.; Starcevic, A. *J. Ind. Microbiol. Biotechnol.* **2014**, *41*, 461−467.
(19) Leitgeb, B.; Szekeres, A.; Manczinger, L.; Vagvolgyi, C.; Kredics, L. *Chem. Biodiversity* **2007**, *4*, 1027−1051.
(20) Ayers, S.; Ehrmann, B. M.; Adcock, A. F.; Kroll, D. J.; Carcache de Blanco, E. J.; Shen, Q.; Swanson, S. M.; Falkinham, J. O., 3rd; Wani, M. C.; Mitchell, S. M.; Pearce, C. J.; Oberlies, N. H. *J. Pept. Sci.* **2012**, *18*, 500−510.
(21) Stoppacher, N.; Neumann, N. K.; Burgstaller, L.; Zeilinger, S.; Degenkolb, T.; Bruckner, H.; Schuhmacher, R. *Chem. Biodiversity* **2013**, *10*, 734−743.
(22) Bills, G.; Li, Y.; Chen, L.; Yue, Q.; Niu, X. M.; An, Z. Q. *Nat. Prod. Rep.* **2014**, *31*, 1348−1375.
(23) Whitmore, L.; Wallace, B. A. *Nucleic Acids Res.* **2004**, *32*, D593−D594.
(24) Berg, A.; Ritzau, M.; Ihn, W.; Schlegel, B.; Fleck, W. F.; Heinze, S.; Grafe, U. *J. Antibiot.* **1996**, *49*, 817−820.
(25) Berg, A.; Schlegel, B.; Ihn, W.; Demuth, U.; Grafe, U. *J. Antibiot.* **1999**, *52*, 666−669.
(26) Lehr, N. A.; Meffert, A.; Antelo, L.; Sterner, O.; Anke, H.; Weber, R. W. *FEMS Microbiol. Ecol.* **2006**, *55*, 105−112.
(27) Karle, I. L.; Flippen-Anderson, J. L.; Agarwalla, S.; Balaram, P. *Proc. Natl. Acad. Sci. U. S. A.* **1991**, *88*, 5307−5311.
(28) Jiao, W. H.; Khalil, Z.; Dewapriya, P.; Salim, A. A.; Lin, H. W.; Capon, R. J. *J. Nat. Prod.* **2018**, *81*, 976−984.
(29) Abarenkov, K.; Zirk, A.; Piirmann, T.; Pöhönen, R.; Ivanov, F.; Nilsson, H. R.; Kõljalg, R. *UNITE Community, 2020*; version 04.02, 2020.
(30) Nguyen, L. T.; Schmidt, H. A.; von Haeseler, A.; Minh, B. Q. *Mol. Biol. Evol.* **2015**, *32*, 268−274.
(31) Kalyaanamoorthy, S.; Minh, B. Q.; Wong, T. K. F.; von Haeseler, A.; Jermiin, L. S. *Nat. Methods* **2017**, *14*, 587−589.
(32) Minh, B. Q.; Nguyen, M. A.; von Haeseler, A. *Mol. Biol. Evol.* **2013**, *30* (5), 1188−1195.
(33) Hoang, D. T.; Chernomor, O.; von Haeseler, A.; Minh, B. Q.; Vinh, L. S. *Mol. Biol. Evol.* **2018**, *35*, 518−522.
(34) Guindon, S.; Dufayard, J. F.; Lefort, V.; Anisimova, M.; Hordijk, W.; Gascuel, O. *Syst. Biol.* **2010**, *59*, 307−321.
(35) Nurk, S.; Bankevich, A.; Antipov, D.; Gurevich, A. A.; Korobeynikov, A.; Lapidus, A.; Prjibelski, A. D.; Pyshkin, A.; Sirotkin, A.; Sirotkin, Y.; Stepanauskas, R.; Clingenpeel, S. R.; Woyke, T.; Mclean, J. S.; Lasken, R.; Tesler, G.; Alekseyev, M. A.; Pevzner, P. A. *J. Comput. Biol.* **2013**, *20*, 714−737.
(36) Camacho, C.; Coulouris, G.; Avagyan, V.; Ma, N.; Papadopoulos, J.; Bealer, K.; Madden, T. L. *BMC Bioinf.* **2009**, *10*, 421.
(37) Blin, K.; Pascal Andreu, V.; de Los Santos, E. L. C.; Del Carratore, F.; Lee, S. Y.; Medema, M. H.; Weber, T. *Nucleic Acids Res.* **2019**, *47*, D625−D630.
(38) Blin, K.; Kim, H. U.; Medema, M. H.; Weber, T. *Briefings Bioinf.* **2019**, *20*, 1103−1113.
(39) Blin, K.; Shaw, S.; Steinke, K.; Villebro, R.; Ziemert, N.; Lee, S. Y.; Medema, M. H.; Weber, T. *Nucleic Acids Res.* **2019**, *47*, W81−W87.

https://dx.doi.org/10.1021/acs.jnatprod.0c01186
J. Nat. Prod. 2021, 84, 1113−1126